Mesoporous Silica Synthesized by Solvent Evaporation: Spun Fibers and Spray-Dried Hollow Spheres

Paul J. Bruinsma,† Anthony Y. Kim, Jun Liu, and Suresh Baskaran*

Pacific Northwest National Laboratory, Mail Stop K2-44, P.O. Box 999, Richland, Washington 99352

Received May 4, 1997. Revised Manuscript Received October 9, 1997⊗

Simple synthesis methods for mesoporous fibers and powders by rapid evaporation of hydrolyzed silicon alkoxide−surfactant solutions are described. Mesoporous fibers are prepared by dry spinning, and mesoporous powders by spray drying of alkoxide−surfactant solutions. Precursor solutions, containing fully hydrolyzed tetraethoxysilane, cetyltrimethylammonium chloride surfactant, and, in the case of the fibers, a fiber-forming polymer, in an acidic alcohol/water mixture, are drawn into continuous filaments or atomized into droplets in a heated air stream. During solvent drying, silica and surfactant self-assemble to form the hexagonally ordered mesophase structure, and all of the nonvolatile components (silica, polymer, and surfactant) are incorporated into the mesophase. The pore diameter and surface area of calcined fibers were 20 Å and 1100 m^2/g, respectively. For the powders, pore sizes of 25 Å and surface areas as high as 1770 m^2/g were measured. Spray-dried powders consisting of hollow spherical particles with mesoporous shells were also produced with this approach.

Introduction

Mesoporous silicate materials properly synthesized with surfactant templates under basic hydrothermal[1,2] and acidic conditions[3] have ordered pores with diameters defined by surfactant micelles. These materials are potentially useful in catalysis, separation, and sensor technologies.[4−6] Recently, Ogawa[7] described a rapid synthesis route for films in which a mixture of tetramethoxysilane hydrolyzed under acid conditions with substoichiometric amounts of water and cetyltrimethylammonium chloride (CTAC) was spin coated on glass substrates. Hexagonally ordered silica film was produced by the solvent evaporation. When cast solutions were dried slowly, poorly ordered materials were formed, indicating the importance of the competition between drying and silica gelation in pore ordering. We have used a similar evaporation approach by spin-coating solutions of tetraethoxysilane (TEOS), ethanol, CTAC, and excess water to obtain mesoporous silica films for low dielectric-constant applications.[8,9] The porosity was well ordered within a narrow concentration range of surfactant,[9] and by varying the surfactant content, the final pore volume could be varied from >0 to 64%. With an analogous dip coating approach, Ganguli et al.[10] have also synthesized mesoporous silica films.

For various applications of mesoporous materials, it will be necessary to control the morphology not only at the nanometer scale of the pore size but also at the micrometer scale. The supported film represents just one example of a defined shape of the mesoporous material. A handful of examples of mesoporous materials with defined morphology have been reported in the literature.[11−16] Lamellar silica with vesicular structure was produced by Tanev and Pinnavaia[11] by hydrolyzing TEOS within multilamellar surfactant vesicles. Schacht et al.[12] utilized TEOS hydrolysis at the oil/water interface with an emulsion. The silica mesophase formed around the oil droplets. With varied stirring conditions, hollow spherical particles to fiberlike particles with up to 1 cm lengths were produced. A related emulsion process was used by Huo et al.[13] to produce mesoporous silica beads with diameters in the millimeter-scale. Nucleation at solid/water[14,15] and air/water interfaces[16] has also been used to produce mesoporous films. Re-

† Present address: Hewlett Packard Co., San Diego, CA 92127.
* Author for correspondence: e-mail s_baskaran@pnl.gov.
⊗ Abstract published in *Advance ACS Abstracts,* November 15, 1997.

(1) Kresge, C. T.; Leonowicz, M. E.; Roth, W. J., Vartuli; J. C.; Beck, J. S. *Nature* **1992**, *359*, 710−712.
(2) Beck, J. S.; Vartuli, J. C.; Roth, W. J.; Leonowicz, M. E.; Kresge, C. T.; Schmidt, K. D.; Chu, C. T.−W.; Olson, D. H.; Sheppard, E. W.; McCullen, S. B.; Higgins, J. B.; Schlenker, J. L. *J. Am. Chem. Soc.* **1992**, *114*, 10834−10843.
(3) Huo, Q.; et al. *Chem. Mater.* **1994**, *6*, 1176−1191.
(4) Raman, N. K.; Anderson, M. T.; Brinker, C. J. *Chem. Mater.* **1996**, *8*, 1682−1701.
(5) Sayari, A. *Chem. Mater.* **1996**, *8*, 1840−1852.
(6) Feng, X.; Fryxell, G. E.; Wang, L.-Q.; Kim, A. Y.; Liu, J.; Kemner, K. M. *Science* **1997**, *276*, 923−26.
(7) Ogawa, M. *J. Chem. Soc., Chem. Commun.* **1996**, 1149.
(8) Liu, J.; Kim, A. Y.; Bontha, J. R.; Baskaran, S. Proceedings of MRS Symposium P, Microporous and Macroporous Materials, April 1996; Materials Research Society: Pittsburgh, PA, in press.
(9) Bruinsma, P. J.; Hess, N. J.; Bontha, J. R.; Liu, J.; Baskaran, S. Low k Mesoporous Silica Films Through Template-Based Processing. Proceedings of the MRS Symposium on Low Dielectric Constant Materials, December 1996; Materials Research Society: Pittsburgh, PA, in press.
(10) Ganguli, R.; Lu, Y.; Anderson, M. T.; Drewiwn, C. A.; Brinker, C. J.; Soyez, H.; Dunn, B.; Huang, M. H.; Zink, J. I. Abstract COL-350, ACS National Meeting; April 13−17, San Francisco, CA 1997.
(11) Tanev, P. T.; Pinnavaia, T. J. *Science* **1996**, *271*, 1267−1269.
(12) Schacht, S.; Hou, Q.; Voigt-Martin, I. G.; Stucky, G. D.; Schueth, F. *Science* **1996**, *273*, 768−771.
(13) Huo, Q.; Feng, J.; Schueth, F.; Stucky, G. D. *Chem. Mater.* **1997**, *9*, 14−17.
(14) Yang, H.; Kuperman, A.; Coombs, N.; Mamiche-Afara S.; Ozin, G. A. *Nature* **1996**, *379*, 703.
(15) Aksay, I. A.; Trau, M.; Manne, S.; Yao, N.; Zhou, L.; Fenter, P.; Eisenberger, P. M.; Gruner, S. M. *Science* **1996**, *273*, 892.
(16) Yang, H.; Coombs, N.; Sokolov, I.; Ozin, G. A. *Nature* **1996**, *381*, 589.

S0897-4756(97)00282-2 CCC: $14.00

cently, Yang et al.[17] have also synthesized an array of mesoporous silica shapes in quiescent solutions of CTAC and hydrolyzed TEOS.

The use of solvent evaporation for mesophase formation is a versatile method for controlling the micrometer scale morphology. In spin coating, excess precursor solution is spun off the substrate, leaving a thin liquid film preform. During drying, a mesophase is formed within the planar film morphology originating from the preform. Here, we describe the fabrication of mesoporous fibers and powders. In the fibers, the micron-scale morphology (fiber diameter) originates from a liquid filament preform. In the powders, particles form from atomized droplets of precursor solutions. Particle morphology depends, in part, on the drying process. Under certain conditions, hollow spheres are produced.

Experimental Section

Fiber Spinning. The spinning solution was formed by combining deionized water, hydrochloric acid (Mallinckrodt), 5×10^6 MW poly(ethylene oxide) (PEO) (Polysciences) from a 4 wt % aqueous stock solution, ethanol (punctilious, Quantum Chemicals), followed by TEOS (Aldrich). The solution was mixed to promote the hydrolysis reaction. Finally, CTAC was added to obtain final mole ratios of 7.0 H_2O, 0.050 HCl, 0.10 PEO (repeat unit), 4.0 ethanol, 1.0 TEOS, 0.24 CTAC. Surfactant with the chloride (rather than bromide) counterion is used, which is known to form hexagonal over lamellar silica mesophases.[6] A thin strand of the viscous solution was drawn from a pipet tip and wound at a rate of 300 m/min onto a spool consisting of six dowels. Fibers were air-dried at 105 °C overnight, and calcined at 600 °C for 3 h.

Spray Drying. The spray-drying solution was formed by combining deionized water, HCl, CTAC, followed by TEOS to obtain final mole ratios of 6.2 H_2O, 0.074 HCl, 0.13 CTAC, 1.0 TEOS for hollow spherical particles and 10.0 H_2O, 0.050 HCl, 0.12−0.28 CTAC, 1.0 TEOS for "collapsed" (described in the Results) particles. The solution was mixed to promote the hydrolysis and then spray-dried in a Buchi 190 Mini Spray Dryer operating with an outlet temperature of 76 °C for hollow spherical particles and 120 °C for collapsed particles. In this formulation, water rather than alcohol dilution is used to avoid possible explosion hazards. Powders were calcined to the same conditions as the fibers.

Characterization. Samples were analyzed by powder X-ray diffraction (PXRD) using a Philips diffractometer with Cu Kα radiation. Pore-size distributions and BET surface areas were determined from N_2 adsorption/desorption isotherms with the Quantachrome Autosorb 6-B gas sorption system, using the BJH[18] and multipoint BET[19] methods, respectively.

Results

Dry-Spun Mesoporous Fibers. Mesoporous fibers were dry spun by drawing the precursor solution into continuous filaments and collecting on a spool. Fibers crossing on the spool during spinning tend to fuse together, creating a gauzelike product between the dowels (see Figure 1). The as-spun fibers are pliable and can be pressed into pellets or rolled into tubes. With drying and calcination the fibers become brittle. Low-temperature oven drying promotes condensation between silica oligomers and increases calcination stability of the mesostructured phase. During calcination, silica undergoes further condensation; surfactant and polymer are removed, leaving the porous structure. The measured mass loss of 59% after calcination is comparable to a value of 57% calculated from the spinning solution composition, assuming the dried fibers contain SiO_2, poly(ethylene oxide) (PEO), and surfactant with chloride bridging ions[3] (for the powders, mass losses were within 1% of the calculated values). The excess loss is attributed to incomplete drying/silica condensation, prior to calcination.

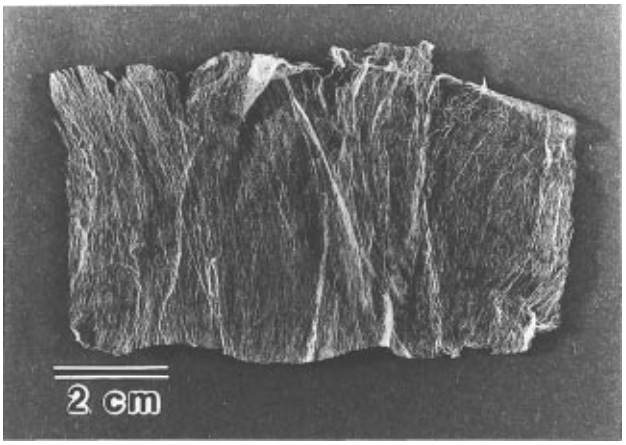

Figure 1. Calcined mesoporous fibers.

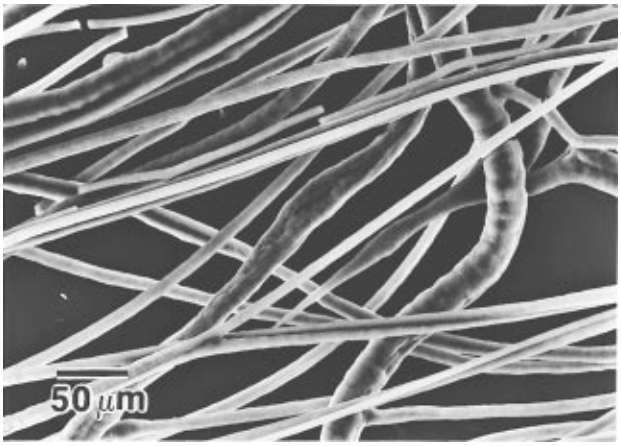

Figure 2. Scanning electron micrograph of the calcined mesoporous silica fibers.

A scanning electron micrograph of these calcined fibers is shown in Figure 2. Fiber diameters are on the order of 40 μm and can be varied by modifying the solution composition and spinning conditions. The distribution of fiber diameters is due to the hand-drawing technique presently used; more uniform fibers would be achieved with state-of-the-art spinning equipment. The fiber cross sections typically have a kidney shape, characteristic of dry-spun fibers where high evaporation rate at the air−fiber interface and comparatively slow solvent diffusion rates through the fiber cause the skin to collapse around the soft cores.[20] Self-assembly of silica and surfactant is believed to occur first at the air−fiber interface, as with film formation at air−water interfaces,[16] followed by progressive conversion of the entire fiber to a mesophase structure. The mesoporous products do not form by the aggregation of preexisting mesoporous particles. Precursor solutions

(17) Yang, H.; Coombs, N.; Ozin, G. A. *Nature* **1997**, *386*, 692−695.
(18) Barrett, E. P.; Joyner, L. G.; Halenda, P. P. *J. Am. Chem. Soc.* **1951**, *73*, 373.
(19) Brunauer, S.; Emmett, P.; Teller, E. *J. Am. Chem. Soc.* **1938**, *60*, 309.
(20) Ziabicki, A. *Fundamentals of Fiber Formation*; Wiley-Interscience: New York, 1976; pp 250−345.

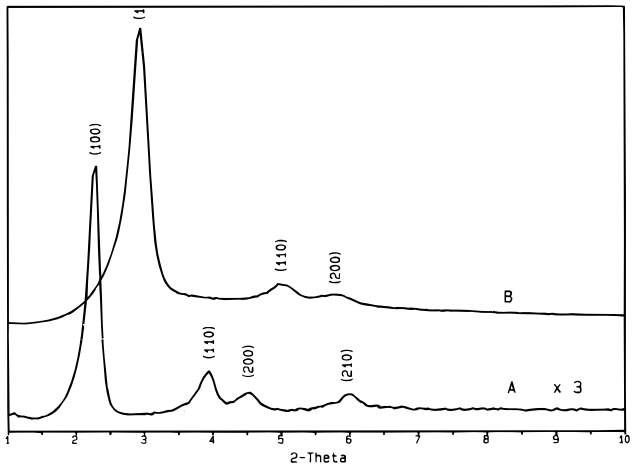

Figure 3. PXRD patterns of mesoporous silica fibers: (A) air-dried fibers; (B) calcined fibers.

are clear, typically stable for several days, and eventually gel rather than form particles, as in the acid-route synthesis of Huo et al.[3]

Powder X-ray diffraction (PXRD) patterns of the dried and calcined fibers are shown in Figure 3. The (100), (110), (200), and (210) reflections corresponding to a hexagonal structure are visible in the PXRD pattern for the dried fibers, although only the first three reflections are visible for the calcined fibers. The increase in peak intensity after calcination (note scale indicated in Figure 3) is due to the greater scattering density contrast and reduced X-ray absorbance after surfactant and polymer removal. The increase is not due to enhancement of pore ordering, since the loss of the (210) reflection, along with a peak-width increase of the (100) reflection, indicates partial loss of order. The d_{100} value of the fibers decreased from 39 to 30 Å on calcination, a 23% decrease comparable to the measured linear shrinkage of 25%.

By nitrogen adsorption/desorption analysis, the mesoporous fibers have a BET surface area of 1100 m^2/g and a 20 Å pore diameter (BJH[18]). Though the pore size is smaller than that of MCM-41 materials,[1,2] primarily as a result of calcination shrinkage, the total surface area is comparable. The adsorption/desorption isotherms show no hysteresis within the resolution of the equipment, indicating that the pores are unconstricted. The hydrophilic PEO polymer, added as a fiber-spinning aid to obtain the proper viscoelastic behavior, is presumably dispersed within the silica phase. The pore volume fraction was 54%, which correlates well with the 57 vol % porosity calculated from the volume contributions of the surfactant and silica phases, after taking into account the volumetric shrinkage measured by the shift in the d_{100} peak. We have shown previously that the pore volume fraction in mesoporous films synthesized by solvent evaporation can be controlled by varying the CTAC/TEOS mole ratio in the precursor solution.[9]

The as-spun, dried and calcined fibers all showed birefringence between cross polarizers in an optical microscope. Consistent with pore orientation along the fiber axis, maximum light transmission occurred with the fiber 45° to the polarizers, and nearly complete extinction occurs when parallel and perpendicular to the analyzer (see Figure 4). Transmission electron microscopy of thin sections of fibers also confirmed pore alignment along the axis. A TEM micrograph (Figure 5) of a thin section from a fiber shows pores aligned in the direction of the fiber axis. This TEM sample was part of a long fragment over 50 μm long, where the ordered cylindrical pores were aligned in the long direction throughout the fragment. Since the fibers were only a few tens of microns in diameter (see Figure 2), the pore direction in this long fragment is most likely along the fiber axis.

When a drop of the precursor solution for the fiber is placed on a microscope slide between cross polarizers, the solution appears initially isotropic. After solvent evaporation for tens of seconds, fanlike hexagonal liquid crystal forms at the three-phase contact line, with micelles preferentially parallel to the contact line. It is this liquid-crystalline phase that is thought to template the silica mesophase.[21,22] We propose that the pore orientation in the fiber also results from a boundary condition, as observed by Ganguli et al.[10] and Yang et al.[16] for films, in which the micelles lie parallel to the air/water interface. In the fibers, the axial micelle orientation represents a lower energy configuration. Axial orientation has been observed previously in elogated mesoporous silica grown in solution[12,17] and in nematic liquid crystals confined in cylindrical pores.[23]

Spray-Dried Mesoporous Powders. In spray drying the particle morphology is dependent on the precursor solution composition and drying conditions. A scanning electron micrograph of mesoporous silica powder consisting of hollow spheres is shown in Figure 6. This particular morphology arises from the formation of a rigid crust, prior to the outward diffusion of the bulk of the solvent from the interior, during drying. From folded sections of collapsed spheres, the shell thickness is estimated to be less than 0.5 μm.

By nitrogen absorption, the BET surface area was 960 m^2/g. Adsorption/ desorption curves showed no hysteresis and indicate a pore size of 19 Å. PXRD patterns of the calcined powder show two broad diffraction peaks that can be indexed to the (100) and (110) reflections corresponding to a weakly ordered hexagonal array (d_{100} = 34 and 31 Å, before and after calcination, respectively). Mesoporous hollow spherical particles may have applications in microencapsulation as suggested by Schacht et al.[12] However, it has not yet been determined whether the pores within the silica shell of the spray-dried powders permit mass transfer between the exterior and interior of the particles.

In a series of experiments, powders were spray-dried from dilute precursor solutions at 120 °C. The surfactant-to-silica mole ratio was varied between 0.12 and 0.28. As shown in the SEM of Figure 7, particle morphology is similar to that of the hollow spheres, except the walls have collapsed during drying. In spray drying, the operating conditions and solution/slurry characteristics can be modified to vary the particle morphology from solid spherical particles to collapsed particles to hollow particles.[24]

(21) Attard, G. S.; Glyde, J. C.; Goeltner, C. G. *Nature* **1995**, *378*, 366−368.
(22) Dabadie, T.; Ayral, A.; Guizard, C.; Cot, L.; Lacan, P. J. *Mater. Chem.* **1996**, *6*, 1789.
(23) Crawford, G. P.; Steele, L. M.; Ondris-Crawford, R.; Iannacchione, G. S.; Yeager, C. J.; Doane, J. W.; Finotello, D. *J. Chem. Phys.* **1992**, *96*, 7788.

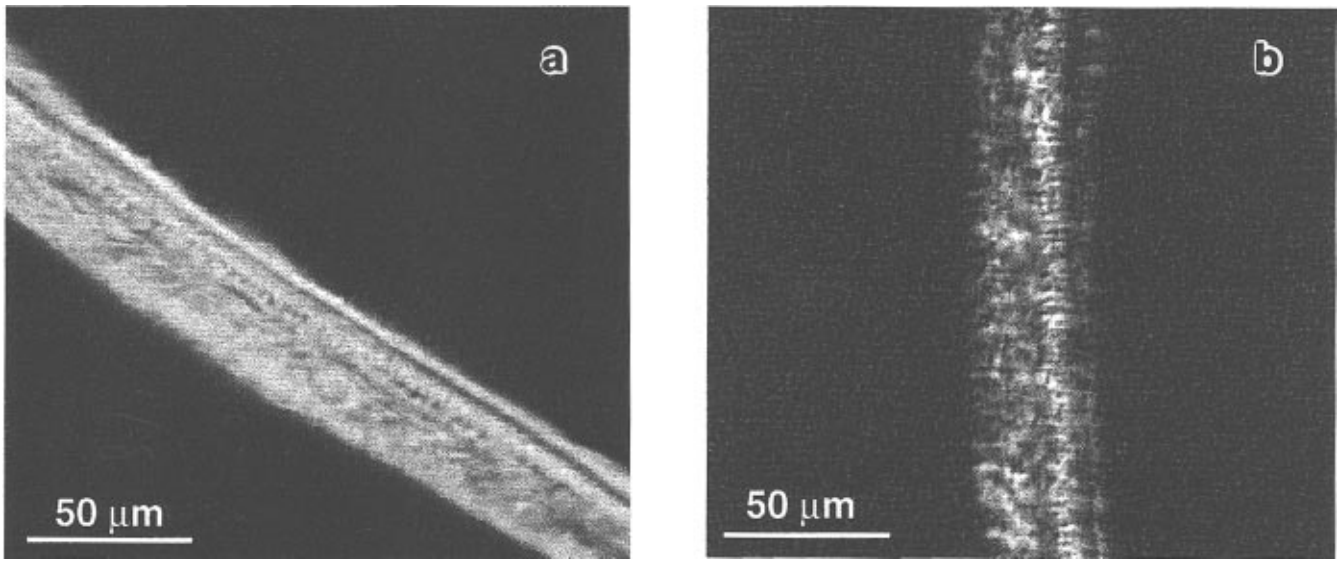

Figure 4. Cross-polarized optical microscopy of a calcined fiber with the fiber axis (a) 45° to the polarizers and (b) parallel and perpendicular to the polarizers.

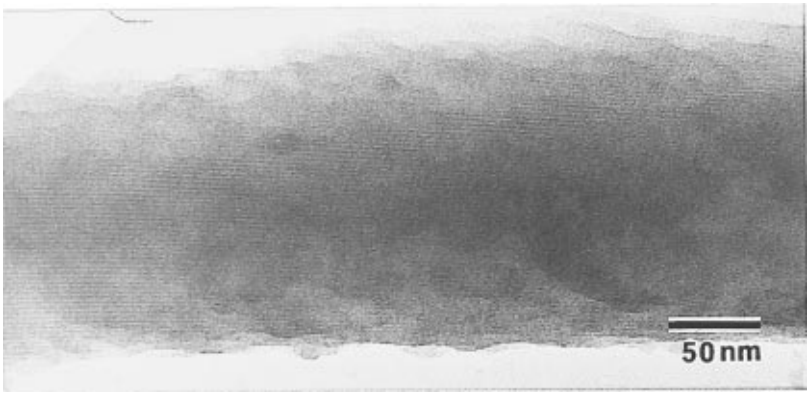

Figure 5. TEM micrograph of mesoporous silica fiber.

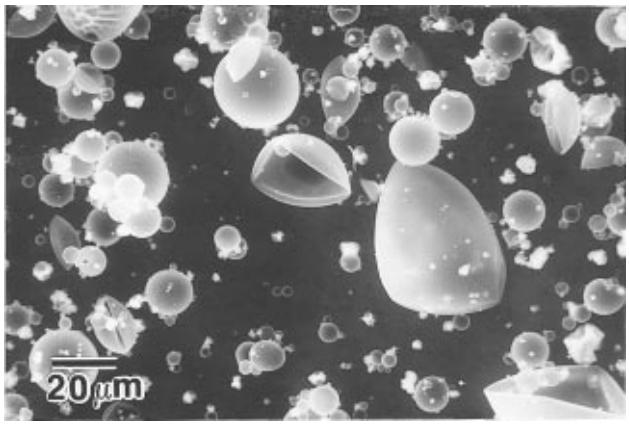

Figure 6. Scanning electron micrograph of the calcined mesoporous hollow spheres produced by spray drying.

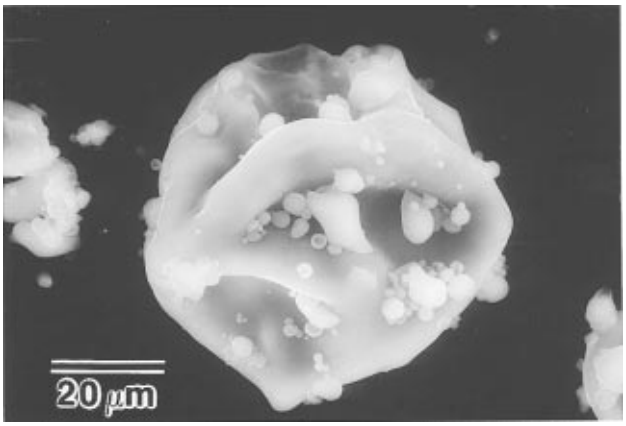

Figure 7. Scanning electron micrograph of the calcined mesoporous collapsed particles produced by spray drying a precursor solution with a surfactant to silica mole ratio of 0.24.

Pore volume fraction and the surface area as a function of surfactant concentration are shown in Figure 8. A maximum pore volume fraction of 63% (37 vol % silica) and a BET surface area up to 1770 m^2/g were achieved at the highest surfactant concentration. The measurement was repeated twice to confirm the high surface area values. The corresponding adsorption/desorption isotherms and the BJH pore size distribution are shown in Figure 9. Nitrogen adsorption/desorption curves show no hysteresis. Samples had a median pore size of approximately 25 Å for all surfactant concentrations, but the isotherms also suggest that pores less than 15 Å may be present. In the PXRD patterns for all calcined powders in this series, the (100), (110), and (200) reflections corresponding to a hexagonal array are evident (see Figure 10). Prior to calcination the (210) reflections are also visible. Interestingly, the d_{100} values are relatively constant with surfactant concentration (~38 Å as synthesized and ~32 Å after calcination).

(24) Masters, K. *Spray Drying Handbook*, 5th ed.; Longman Scientific & Technical: Harlow, Essex, England, 1991; pp 335−336.

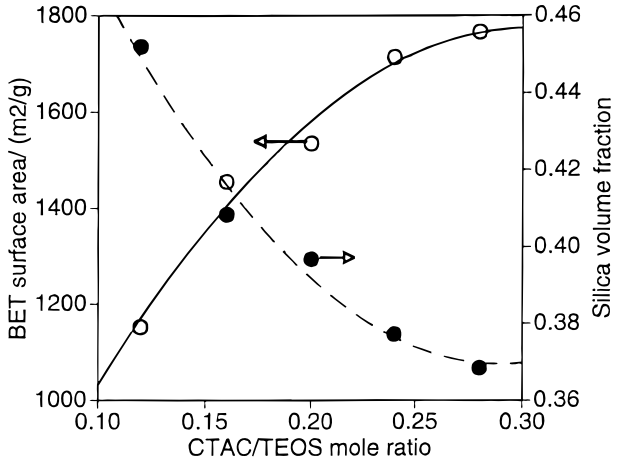

Figure 8. Pore volume fraction and surface area of calcined spray-dried powders as a function of the surfactant-to-silica mole ratio.

Finally, experiments to incorporate aluminum in the spray dried powders by the addition of aluminum chloride to the precursor solutions were also carried out. For an aluminum-to-silica mole ratio of 1:16, the aluminum in the as-synthesized powders was predominately framework, as determined by ^{27}Al NMR. However, the framework substitution was not retained upon calcination.

Discussion

In the rapid solvent evaporation method described in this paper, preforms are obtained by essentially mechanical means, resulting in good control of the micrometer-scale morphology in the mesostructured product. During solvent drying, silica and surfactant self-assemble to form the mesophase structure, and all of the nonvolatile components (silica, surfactant, and polymer) are incorporated into the fibers and powders. No aqueous surfactant solution remains as a byproduct; mesophase material is produced without filtration. The mesophase is formed rapidly in seconds, or even in fractions of a second in spray drying. Because there is no partitioning with an aqueous solvent, the surfactant-to-silica mole ratio in the mesophase, at least on average, is determined by the precursor solution composition.

In fiber spinning, high molecular weight PEO was added to allow spinning. This introduces the general possibility of using soluble polymers to modify the rheological properties of the precursor solution. Control over rheology would be useful in the extension of this method to other processes, such as doctor blading and screen printing, in which shear-thinning solutions are desirable.

Synthesis routes based on aging/gelation of silica oligomers within a lyotropic liquid-crystal phase have been widely studied.[21,22] The evaporation method described here differs because the composition and temperature of the precursor solution change over short periods of time. However, the evaporation and aging/gelation method share many common aspects. In the evaporation method, the mesophase formation involves the formation of a lyotropic liquid-crystalline phase from an initially isotropic sol. At some stage in the drying, the lyotropic phase is "locked-in" either by diffusion barriers or by silica gelation. To form an ordered lytropic phase, Attard et al.[21] found it was necessary to apply a light vacuum to remove the alcohol resulting from alkoxide hydrolysis. In the evaporation method, preferential evaporation of the more volatile alcohol over water must also have a role in the micelle formation and ordering.

Because of the time dependencies and gradients of temperature and composition, the mesophase formation is a complex, path-dependent process. Our strategy for forming hexagonally ordered mesophase with each preform method (i.e., in spin coating, fiber spinning, or spray drying) involves determination of the optimum precursor chemistry, primarily by systematic variation of the surfactant content in the precursor solution, to obtain ordered mesoporous products. With this rapid evaporation approach, alcohol, produced as a hydrolysis byproduct or added as a diluent, may also affect the mesophase structure simply by evaporative cooling.

During spray drying, solvent evaporation leads to increased concentrations of the surfactant and silica oligomers, and the solution undergoes transitions from spherical micelles, to rod-shaped micelles, to hexagonal mesostructures.[10] However, the residence time within the drying column of the spray drier is estimated to be 0.2 s. Therefore, the mesophase structure forms extremely rapidly, and the possible kinetic limitations to surfactant phase transitions must be considered. Rapid drying may also limit the distance over which the micelle orientations are correlated.

The conditions of mesophase formation are not uniform throughout the preform as a consequence of the drying process. Although PXRD patterns indicate well-ordered hexagonal phases, and the nitrogen adsorption/desorption curves indicate narrow size distributions, the presence of gradients in the mesophase structure cannot be ruled out without further characterization. The present results may indicate structural gradients in the spray-dried powders. The surface area and pore volume fraction increase with surfactant content. However, the d_{100} values from the PXRD patterns and the pore sizes remain relatively constant. In spin-coated films[9] and the fibers, the pore volume fraction can be rationalized in terms of the volume contributions of surfactant and silica. In the spray-dried powders, the actual pore volume fractions fall short of the values calculated from the precursor solution compositions. These observations may indicate a mixture of mesoporous and nonporous regions within the spray-dried particles.

The rapid evaporation method described in this paper differs from the traditional aqueous route,[3] where surfactants and silicates are mixed in a solution and aggregate structures are formed immediately. In the traditional aqueous route, the binding between the organic and inorganic species is determined by charge density matching.[3] Condensation of the inorganic species leads to a change in the charge density at the interface and to a phase transformation if the reaction conditions occur near a phase boundary. The evaporation method described in this work avoids the phase partitioning that occurs in the traditional aqueous synthesis method. The amount of silicate and surfactant that can be incorporated into the mesostructure is not determined by charge density matching. This offers more flexibility in controlling the properties of the

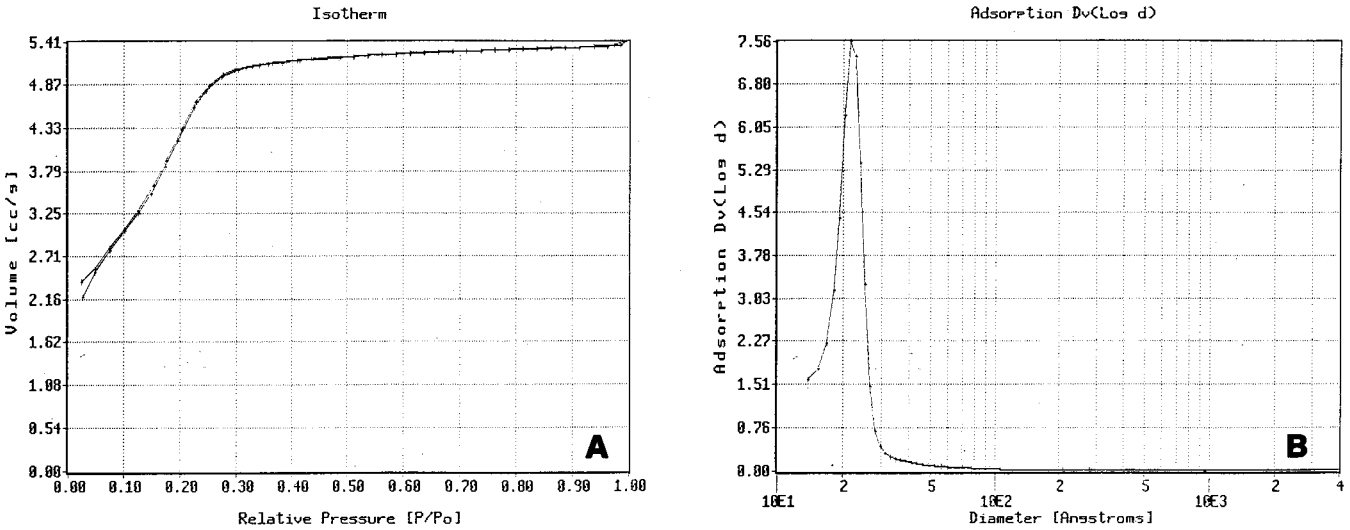

Figure 9. Nitrogen adsorption/desorption isotherms (A) and pore-size distribution (B) for collapsed mesoporous particles produced by spray drying.

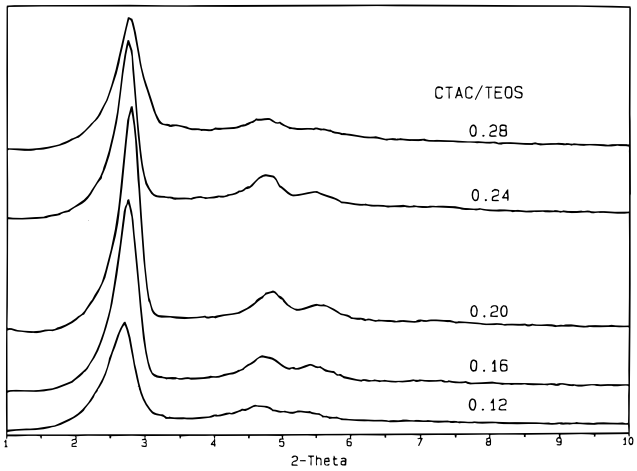

Figure 10. PXRD patterns of calcined spray-dried powders for different surfactant-to-silica mole ratios.

mesoporous product, as for example, in tailoring the pore volume with surfactant concentration.

Conclusions

A process was demonstrated for the rapid fabrication of well-ordered mesoporous material with a true fiber morphology, and pore alignment with the fiber axis. Spray-dried mesoporous powders were also produced with structures ranging from hollow spheres to collapsed particles. The mesophase in these structures forms by self-assembly during rapid drying of solvent. In spray drying, the cooperative organization to form the mesophase structure occurs in a fraction of a second. The mesophase retains some characteristic of the preform shape (i.e., the atomized droplet or liquid filament). Morphology can also be dependent, in part, on the drying conditions, as is evident by noncircular fiber cross sections and the different particle types achieved by spray drying. The fibers and powders are produced rapidly and with relative ease, as compared to previous mesophase synthesis methods. The evaporation method may have advantages in the fabrication of mesoporous materials and engineered supports for large-scale processes. The fibers, for example, can be wound into a fiber module as an engineered catalyst support. In addition to fibers, powders, and thin films, this method can potentially be extended to create a variety of other useful engineered mesoporous materials.

Acknowledgment. P.J.B. was supported in this research by Associated Western Universities, Inc., Northwest Division under Grant DE-FG06-92RL-12451 with the U.S. Department of Energy. Additional support was provided by the USDOE Office of Transportation Technology. Pacific Northwest National Laboratory is operated for the U.S. Department of Energy by the Battelle Memorial Institute under Contract DE-AC06-76RLO 1830.

CM970282A